TECHNISCHE MECHANIK, 32, 2-5, (2012), 507 – 517
submitted: November 1, 2011

Modelling of Thin Films of Shape-Memory Alloys

G. Pathó

After a brief introduction to the physical and mathematical problem related—not only—to shape-memory alloys and a review of different variational models for thin martensitic films, a numerical approach based on the first laminate is proposed, followed by computational experiments.

1 Introduction

Shape-memory alloys (SMAs) have been subject to extensive theoretical and experimental research since the last half a century—when the martensitic phase transformation was first explained in the AuCd alloy in 1951.

This non-diffusive, solid-to-solid phase transformation leads to a change in the crystallographic structure of the material. The SMAs exist in two phases: at high temperature the austenite phase (having one crystallographic configuration with high symmetry—usually cubic structure) while lower temperatures lead to a low-symmetric grid, e.g., tetragonal, orthorhombic, monoclinic, which is then called martensite phase and may occur in M different variants (here $M = 3, 6, 12$ for the cases mentioned above).

Shape-memory alloys belong to the group of intelligent materials: they do not only have the ability to detect changes of their environment—stress and temperature, in particular—but they are also able to react to these changes. Furthermore, this behaviour being induced by the mere transformation of the crystallographic lattice of the alloy, the size of an SMA component can be reduced significantly—up to the order of $10\ \mu m$—without affecting its functionality.

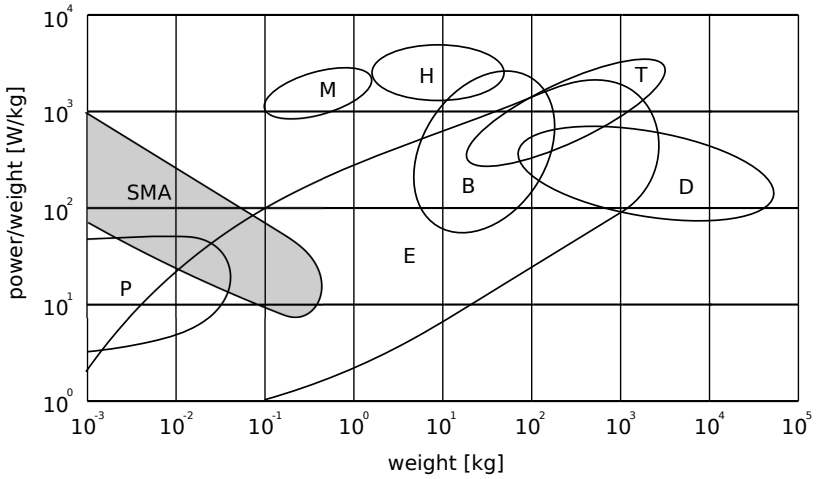

Figure 1: Power–weight ratio for different types of actuators; P – piezoelectric transducers, E – electromotors, M – modeller motors, H – hydraulic motors, B – piston gas-engines, D – piston diesel-engines, T – internalcombustion turbines, SMA - shape-memory alloy actuators (picture in accordance with Figure 6 of Šittner and Novák (2002))

Due to this delicate feature, miniature components made of shape-memory alloys have found numerous applications in many different areas of science and technology from microrobotics to thin films—particularly the sputter-deposited NiTi thin films, which are widely used as microactuators in the micro-electro-mechanical systems (MEMS), e.g., cantilevers, diaphragms, micropumps, microvalves, dumpers (cf. Pan and Cho (2007) for the demonstration of such a dumper), different grippers, springs or mirror actuators. For an extensive overview of the

modern decomposition techniques, key engineering characteristics and applications of NiTi thin films cf. Miyazaki et al. (2009).

2 Mathematical Model of SMA Static Problems in 3D

In what follows L^p will denote the standard Lebesgue space of measurable mappings which are integrable with the p-th power for $1 \leq p < +\infty$ or essentially bounded for $p = +\infty$. Further, $W^{k,p}$ will stand for the Sobolev space of mappings belonging together with their derivatives up to the order k to L^p.

Usually, the formulation of the mathematical minimization problem related to the static description of bulk shape-memory alloys at a given temperature θ is

$$\begin{aligned} &\text{Minimize} \quad \mathcal{I}(y) = \int_\Omega \varphi(\nabla y(x))\,\mathrm{d}x \\ &\text{subject to} \quad y \in \mathfrak{A}_{y_0}, \end{aligned} \tag{1}$$

where y is the deformation of the reference configuration $\Omega \subset \mathbb{R}^3$, Ω open bounded domain, furthermore, the set $\mathfrak{A}_{y_0} := \left\{ w \in W^{1,p}(\Omega, \mathbb{R}^3) : \det \nabla w > 0 \text{ a.e. in } \Omega,\ w|_{\Gamma_0} = y_0 \right\}$ denotes the set of admissible deformations with $1 < p < +\infty$ and y_0 defining a suitable Dirichlet boundary condition on a prescribed $\Gamma_0 \subset \partial\Omega$, $\mathrm{meas}(\Gamma_0) > 0$ such that $\mathfrak{A}_{y_0} \neq \emptyset$.

The Helmholtz free energy density $\varphi\colon \mathbb{R}^{3\times 3} \to \mathbb{R}$ is a continuous function defined on the set of real 3×3 matrices obliging the physical property of material frame-indifference, more precisely

$$\varphi(QF) = \varphi(F) \qquad \forall Q \in SO(3), \tag{2}$$

where $SO(3) = \{Q \in \mathbb{R}^{3\times 3} :\ Q^T Q = Q Q^T = I,\ \det Q = 1\}$ denotes the set of all rotations and I the 3×3 identity matrix.

Without loss of generality let us consider the energy density normalized, so that $\varphi \geq 0$. Then different variants of the particular phases are modelled through the multi-well structure of φ, i.e.,

$$\varphi(F) = 0 = \min_{\mathfrak{A}_{y_0}} \varphi(\cdot) \quad \Leftrightarrow \quad F \in \mathcal{A} \cup \mathcal{M}, \tag{3}$$

where $\mathcal{A} := SO(3)U_0$, resp. $\mathcal{M} := SO(3)U_1 \cup SO(3)U_2 \cup \cdots \cup SO(3)U_M$ stands for all the matrices related to the austenitic phase, resp. the martensitic phase (consisting of M variants)—bearing in mind the frame-indifference of the stored energy density, too—the particular matrices U_0, resp. $U_1, \ldots U_M$ are then the so called Bain matrices of the austenite, resp. martensite.

Furthermore, the energy density should satisfy the growth condition

$$c(|A|^p - 1) \leq \varphi(A) \leq C(1 + |A|^p) \qquad \forall A \in \mathbb{R}^{3\times 3} \tag{4}$$

for some $c, C \in \mathbb{R}$.

Due to the multi-well character of φ—implying its lack of quasiconvexity—(1) may not admit any solution in the class of Sobolev spaces as for any minimizing sequence is allowed to—and does for certain conditions on y_0 and between U_i—develop finer and finer oscillations between the wells.

Let us recall that a function $g\colon \mathbb{R}^{m\times n} \to \mathbb{R}$ is quasiconvex if the inequality

$$g(A) \leq \frac{1}{|\mathcal{O}|} \int_{\mathcal{O}} g(A + \nabla\psi(x))\,\mathrm{d}x \tag{5}$$

holds valid for any $A \in \mathbb{R}^{m\times n}$ and any $\psi\colon \mathcal{O} \to \mathbb{R}^m$ smooth, where $\mathcal{O} \subset \mathbb{R}^n$ is an open domain (in fact, the property of quasiconvexity is independent of the chosen domain $\mathcal{O}$).

Two procedures have been proposed to overcome the aforementioned problem of non-existence of classical Sobolev minimizers to (1). Dacorogna (1989) showed that one can extend the functional $\mathcal{I}$ to a relaxed functional $\mathcal{I}_Q$

which defines a minimization problem delicately related to the initial one but exhibiting a solution in the related Sobolev space, cf. the last paragraph, the first equality in (10), in particular. Let us recall that the relaxed problem is connected to the quasiconvexification of φ, namely

$$\begin{aligned} &\text{Minimize} \quad \mathcal{I}_Q(y) = \int_\Omega Q\varphi(\nabla y(x))\,\mathrm{d}x \\ &\text{subject to} \quad y \in \mathfrak{A}_{y_0}, \end{aligned} \tag{6}$$

where $Q\varphi$ is the quasiconvex envelope of the energy density, i.e.,

$$Q\varphi = \sup\{\psi\colon \psi \le \varphi,\ \psi \text{ quasiconvex}\}. \tag{7}$$

The other method for introducing a meaningful solution of (1) stems from extending the notion of solution to the objects called gradient Young measures, which are weakly* measurable mappings $x \mapsto \mu_x\colon \Omega \to \mathrm{rca}(\mathbb{R}^{3\times 3})$—i.e., the mapping $\Omega \to \mathbb{R}\colon x \mapsto \langle \mu_x, v\rangle = \int_{\mathbb{R}^{3\times 3}} v(s)\mu_x(\mathrm{d}s)$ is Lebesgue measurable for every continuous function with compact support $v \in C_0(\mathbb{R}^{3\times 3})$—with values in probability measures generated by sequences of gradients of Sobolev maps.

Then defining the set of all gradient Young measures $\mathcal{G}^p$ as

$$\mathcal{G}^p(\Omega;\mathbb{R}^{3\times 3}) = \big\{\mu \in L^\infty_w(\Omega;\mathrm{rca}(\mathbb{R}^{3\times 3})) : \exists\{y_k\}_{k\in\mathbb{N}} \text{ bounded in } W^{1,p}(\Omega;\mathbb{R}^3) \text{ such that } \delta_{\nabla y_k} \overset{*}{\rightharpoonup} \mu\big\}, \tag{8}$$

where δ_x is the usual delta function with support at the point x and the weak* convergence is understood in the dual space $L^\infty_w(\Omega;\mathrm{rca}(\mathbb{R}^{3\times 3})) \simeq L^1(\Omega;C_0(\mathbb{R}^{3\times 3}))^*$—the subscript w indicating the above mentioned weak* convergence of measures—, one is led to formulate the relaxed minimization problem as

$$\begin{aligned} &\text{Minimize} \quad \mathcal{I}_Y(\mu) = \int_\Omega \int_{\mathbb{R}^{3\times 3}} \varphi(s)\mu_x(\mathrm{d}s)\,\mathrm{d}x \\ &\text{subject to} \quad \mu \in \mathcal{G}^p(\Omega;\mathbb{R}^{3\times 3}), \\ &\qquad\qquad\ \ y_\mu \in \mathfrak{A}_{y_0}, \end{aligned} \tag{9}$$

where $y_\mu \in W^{1,p}(\Omega;\mathbb{R}^3)$—called the underlying deformation of the measure μ—is the weak limit of the generating sequence $\{y_k\}_{k\in\mathbb{N}}$ from definition (8).

It can be shown—among others—that

$$\min(6) = \inf(1) = \min(9), \tag{10}$$

whereas any minimizer $y \in \mathfrak{A}_{y_0}$ of (6) admits a minimizing sequence of (1) converging weakly to y in $W^{1,p}(\Omega;\mathbb{R}^3)$ and every minimizer of (9) is generated by gradients of minimizing sequences of (1). The advantage of the Young-measure approach lies in its ability of capturing the microstructure beyond the macroscopic deformation as well. For further details cf. e.g. Dacorogna (1989); Müller (1999); Pedregal (1997); Roubíček (1997).

3 Dimension Reduction

3.1 Limiting Energy Densities

Modelling of thin films of shape-memory alloys relies on a Γ-convergence procedure when going to zero with the material thickness $h > 0$ of the domain $\Omega_h = \omega \times (-h/2, h/2)$, $\omega \subset \mathbb{R}^2$ open and bounded. In order to do so one transforms the total energy $I_h(y)$ to a scaled integral of a reference configuration $\Omega_1 = \omega \times I$, $I := (-1/2, 1/2)$, not depending on h by a scaling factor of $1/h$; cf. Friesecke et al. (2006) for a hierarchy of different nonlinear plate theories arising from different scaling of the free energy and the power of external forces.

More precisely, one is looking for the variational limit

$$\lim_{h\to 0_+} I_h(y) = \lim_{h\to 0_+} \frac{1}{h} \int_{\omega\times I} \varphi\Big(\nabla_p y(x)\Big|\frac{1}{h}\nabla_3 y(x)\Big)\,\mathrm{d}x, \tag{11}$$

where the expressions $\nabla_p y \in \mathbb{R}^{3\times 2}$, resp. $\nabla_3 y \in \mathbb{R}^3$ denote the planar gradient of y, i.e., the gradient of $y = y(x_p)$, $x_p = (x_1, x_2)$, resp. the partial derivative of $y = y(x)$ in the direction e_3 perpendicular to the basis $\{e_1, e_2\}$ of the film ω; the notation $(A|a_3)$ for a 3×2 matrix A with columns a_1 and a_2 means then the 3×3 matrix $\sum_{i=1}^{3} a_i \otimes e_i$.

The first rigorous results were due to Le Dret and Raoult (1995) who obtained the limit functional

$$\mathcal{I}_{\mathcal{LDR}}(y) = \int_\omega Q\varphi_0(\nabla_p y)\,\mathrm{d}x_p, \tag{12}$$

which involved $Q\varphi_0$ the quasiconvex envelope of the effective energy density φ_0 defined for $F \in \mathbb{R}^{3\times 2}$ as

$$\varphi_0(F) = \min_{z\in\mathbb{R}^3} \varphi(F|z), \tag{13}$$

capturing well the average macroscale deformation of the material but with the obvious drawback of losing the finer scale oscillations of the deformation gradient forming the structure of laminates.

For this purpose gradient Young measures introduced above should be taken into account when determining the Γ–limit of the total energy functionals. Freddi and Paroni (2004) arrived at the following expression

$$\mathcal{I}_{\mathcal{FP}}(\mu) = \int_\omega \int_{\mathbb{R}^{3\times 2}} \varphi_0(F)\,\mathrm{d}\mu_{x_p}\,\mathrm{d}x_p, \tag{14}$$

where $\mu \in L^\infty_w(\omega; \mathrm{rca}(\mathbb{R}^{3\times 2}))$. In addition, they have shown a certain uniqueness of the limiting stored energy density, i.e., that among all continuous integrands with p-th growth φ_0 is the sole function the Young-measure relaxation of which is equal to $\mathcal{I}_{\mathcal{FP}}$ for every linear boundary condition. More precisely, if denoting

$$W^{1,p}_A(\omega;\mathbb{R}^3) = \{w \in W^{1,p}(\omega;\mathbb{R}^3)\colon w(x) = Ax \text{ on } \gamma_0 \subset \partial\omega,\ \mathrm{meas}(\gamma_0) > 0\} \tag{15}$$

for a real matrix $A \in \mathbb{R}^{3\times 2}$ and let, on one hand, $Q[\mathcal{I}_\psi, A]$ be the relaxation, i.e., the lower-semicontinuous envelope, of

$$\mathcal{I}_\psi(y) = \int_\omega \psi(\nabla_p y)\,\mathrm{d}x_p, \tag{16}$$

where $\psi\colon \mathbb{R}^{3\times 2} \to \mathbb{R}$ is continuous with p-th growth, cf. (4) with $A \in \mathbb{R}^{3\times 2}$, on $W^{1,p}_A(\omega;\mathbb{R}^3)$ with respect to the weak topology, and $Y[\mathcal{I}_\psi, A]$ be the relaxation of

$$\mathcal{I}^*_\psi(\nu) = \begin{cases} \mathcal{I}_\psi(y) & \text{if } \nu = \delta_{\nabla_p y} \text{ for some } y \in W^{1,p}_A(\omega;\mathbb{R}^3), \\ +\infty & \text{otherwise in } L^\infty_w(\omega; \mathrm{rca}(\mathbb{R}^{3\times 2})) \end{cases} \tag{17}$$

with respect to the weak* topology of $L^\infty_w(\omega; \mathrm{rca}(\mathbb{R}^{3\times 2}))$. Then it can be shown that

$$\mathcal{I}_{\mathcal{LDR}}(y) = Q[\mathcal{I}_{\varphi_0}, A](y) \quad \text{and} \quad \mathcal{I}_{\mathcal{FP}}(\mu) = Y[\mathcal{I}_{\varphi_0}, A](\mu). \tag{18}$$

Furthermore, for all $A \in \mathbb{R}^{3\times 2}$ it holds that

$$Y[\mathcal{I}_\psi, A] = Y[\mathcal{I}_{\varphi_0}, A] \quad \Rightarrow \quad \psi \equiv \varphi_0. \tag{19}$$

cf. Freddi and Paroni (2004), Section 7 for more details. Note that an analogue does not hold in the case of $\mathcal{I}_{\mathcal{LDR}}$ as there are infinitely many functions with a quasiconvex envelope equal to $Q\varphi$.

Another approach was chosen by Bhattacharya and James (1999) who considered the total energy as the Helmholtz free energy augmented with an interfacial energy, a term penalizing the oscillations of the deformation gradient between different phases (as real materials do not develop inifinitely fine-scale lamination either), namely, $I_h(y)$ of the form

$$I_h(y) = \int_{\Omega_h} \varphi(\nabla y) + \kappa|\nabla^2 y|^2\,\mathrm{d}x, \tag{20}$$

where $\kappa > 0$ taken small but fixed. This additional term—yielding a smoothing effect—results in a limit energy density which needs no relaxation, an interfacial term still present, though, namely

$$\mathcal{I}_{\mathcal{BJ}}(y,b) = \int_\omega \varphi(y_{,1}|y_{,2}|b) + \kappa^2\{|\nabla_p^2 y|^2 + 2|\nabla_p b|^2\}\,\mathrm{d}x_p. \tag{21}$$

Note that the deformation of the thin film is described by two vector fields, $y\colon \omega \to \mathbb{R}^3$ holding the information about the mid-plane deformation of the film and $b\colon \omega \to \mathbb{R}^3$ outlining the behaviour of the cross-section of the film under loading.

One year later it was Shu (2000) who showed that if κ is also taken dependent on the material thickness $\kappa = \kappa(h)$ then the limit functional $\mathcal{I}_{\mathcal{LDR}}$ may be recovered for $h \to 0_+$ and $\kappa(h) \to 0_+$—independently of the ratio κ/h.

More recently, in order to derive rigorously a limiting thin film theory in the absence of an interfacial term while still recovering the aforementioned Cosserat vector field b Bocea (2007) introduced the scaled gradient Young measures, which are Young measures generated by sequences of scaled gradients of the form $\left\{\left(\nabla_p w_k \middle| \frac{1}{h_k}\nabla_3 w_k\right)\right\}_{k\in\mathbb{N}}$, $h_n \to 0_+$.

When defining the set of all scaled gradient Young measures with underlying deformation $y \in W^{1,p}(\Omega;\mathbb{R}^3)$ and associated Cosserat vector $b \in L^p(\Omega;\mathbb{R}^3)$ as

$$\mathcal{G}^p_{y,b}(\Omega;\mathbb{R}^{3\times 3}) := \Bigg\{\mu \in L^\infty_w(\Omega;\mathbb{R}^{3\times 3}) \;\Bigg|\; \exists h_n \to 0_+\ \exists\{y_n\} \subset W^{1,p}(\Omega;\mathbb{R}^3):$$
$$y_n \rightharpoonup y, \quad \frac{1}{h_n}\nabla_3 y_n \rightharpoonup c, \quad \delta_{\left(\nabla_p y_n \middle| \frac{1}{h_n}\nabla_3 y_n\right)} \overset{*}{\rightharpoonup} \mu\Bigg\}, \tag{22}$$

where the weak convergences are taken subsequently in the spaces $W^{1,p}(\Omega;\mathbb{R}^3)$, $L^p(\Omega;\mathbb{R}^3)$ and the dual space $L^\infty_w(\Omega;\mathrm{rca}(\mathbb{R}^{3\times 3}))$, respectively, then the following assertion for the asymptotic limit holds:

$$\mathcal{I}_{\mathcal{B}}(y,b) = \min_{\mu\in\mathcal{G}^p_{y,c}(\Omega;\mathbb{R}^{3\times 3})} \int_\Omega \varphi\,\mathrm{d}\mu. \tag{23}$$

This results from the decomposition of the sequence of scaled gradients into a p-equiintegrable part carrying the oscillations and a remainder accounting for the concentrations (but converging to zero in measure), cf. Bocea (2008); Bocea and Fonseca (2002); Braides and Zeppieri (2007). However, the set of scaled gradient Young measures still lacks any effective analytical description analogous to the one of gradient Young measures by Kinderlehrer and Pedregal (1994).

3.2 Compatibility Condition for the Deformation

In what follows, we will concentrate on the thin-film model proposed by Bhattacharya and James (1999) in order to implement it and make numerical simulations for a NiMnGa alloy.

For a deformation which does not tear the film apart, the Hadamard jump condition ought to be satisfied, which turns out to be essentially different from the bulk case. This condition requires in the thin film theory the existence of an invariant line interface between two (suitably rotated) zero-energy deformation gradients under a given deformation (the deformation gradient and the Cosserat vector may, however, suffer jumps across the interface). More precisely, let $\omega = \omega_1 \cup \omega_2 \cup \mathcal{L}$, where ω_1 and ω_2 are two disjoint subsets and $\mathcal{L}$ is a line segment between them. Then, if

$$(y_{,1}|y_{,2}|b) = \begin{cases} Q_1 U & \text{in } \omega_1 \\ Q_2 V & \text{in } \omega_2, \end{cases} \tag{24}$$

y denoting the deformation, b the associated Cosserat vector, while $U \neq V$ are two Bain matrices, Bhattacharya and James (1999) showed that the thin-film twinning equation may be expressed as

$$QU - V = a \otimes n + c \otimes e_3, \tag{25}$$

for suitable $Q \in SO(3)$, $a, n, c \in \mathbb{R}^3$ such that $n \cdot e_3 = 0$. Note that this condition is much weaker than the one required in 3D, i.e., rank$(QU - V) = 1$, which predicts the need of a planar interface between the energy wells. As a consequence, there might exist interfaces between particular phases in thin films which do not in the bulk material. E.g., there are certain materials which may exhibit a sharp interface between the austenite and the martensite, this phenomenon being theoretically impossible in the 3D setting.

4 Numerical Experiments

4.1 Sequential Laminates

Due to the non-local character of quasiconvexity it is difficult in most of the cases to compute the quasiconvex envelope of a particular function explicitly.

Therefore, one is pursuaded to consider a more general type of convexity, namely, the rank-one convexity which is defined as the property of a function $f\colon \mathbb{R}^{m\times m} \to \mathbb{R}$ being convex along rank-one connected matrices, i.e.,

$$f(\lambda A + (1-\lambda)B) \leq \lambda f(A) + (1-\lambda) f(B) \quad \text{whenever} \quad \text{rank}(A-B) \leq 1 \text{ and } 0 \leq \lambda \leq 1. \tag{26}$$

When introducing the rank-one convex envelope, analogously to the quasiconvex envelope, as

$$R\varphi = \sup\{\psi\colon \psi \leq \varphi,\ \psi \text{ rank-one convex}\} \tag{27}$$

one can easily see that it provides an upper bound for the quasiconvex envelope

$$Q\varphi \leq R\varphi \leq \varphi. \tag{28}$$

A useful approximation procedure of this envelope is proposed by Kohn and Strang (1986), namely

Proposition 1. (see (Kohn and Strang, 1986, II)) Let $f\colon \mathbb{R}^{3\times 3} \to \mathbb{R}^3$ be bounded from below, then for every $A \in \mathbb{R}^{3\times 3}$ it holds that

$$Rf(A) = \lim_{k\to+\infty} R_k f(A), \tag{29}$$

where

$$R_0 f(A) = f(A), \tag{30}$$

then subsequently for $k = 1, 2, \ldots$

$$R_k f(A) = \inf_{(\lambda, A_0, A_1)\in \mathcal{M}_A} \big(\lambda R_{k-1} f(A_0) + (1-\lambda) R_{k-1} f(A_1)\big), \tag{31}$$

$R_k f$ called k-th order laminate, and the set of admissible microstructures $\mathcal{M}_A \subset [0,1] \times \mathbb{R}^{3\times 3} \times \mathbb{R}^{3\times 3}$ for the matrix A defined as

$$\mathcal{M}_A = \{(\lambda, A_0, A_1)\colon A = \lambda A_0 + (1-\lambda) A_1 \text{ and } \text{rank}(A_1 - A_0) \leq 1\}. \tag{32}$$

Hence, utilizing this latter characterization of rank-one convex envelope one can state the minimization problem for $k \in \mathbb{N}$ as

$$\begin{aligned} &\text{Minimize} \quad \mathcal{I}_{R_k}(y) = \int_\Omega R_k\varphi(\nabla y(x))\,\mathrm{d}x \\ &\text{subject to} \quad y \in \mathfrak{A}_{y_0}, \end{aligned} \tag{33}$$

and observe that

$$\min (6) = \inf (33) = \inf (1) \tag{34}$$

for all $k \in \mathbb{N}$, which follows from the inequality $Q\varphi \leq R\varphi \leq \cdots \leq R_2\varphi \leq R_1\varphi \leq \varphi$ and relation (10).

In our simulations the first order laminate was used to approximate the rank-one convex envelope of the free energy density (21) while considering the contribution of the interfacial energy negligible, therefore setting the interfacial parameter $\kappa = 0$.

In order to set the numerical model let us first, by combining the thin-film twinning equation and the expression for the first order laminate, i.e.,

$$\begin{aligned} (y_{,1}|y_{,2}|b) &= \lambda A_0 + (1-\lambda)A_1, \\ A_1 - A_0 &= a \otimes n + c \otimes e_3, \end{aligned} \tag{35}$$

for some $a, n, c \in \mathbb{R}^3$ such that $n \cdot e_3 = 0$, express

$$\begin{aligned} A_0 &= (y_{,1}|y_{,2}|b) - (1-\lambda)(a \otimes n + c \otimes e_3), \\ A_1 &= (y_{,1}|y_{,2}|b) + \lambda(a \otimes n + c \otimes e_3). \end{aligned} \tag{36}$$

Furthermore, let us consider the finite element discretization, more precisely element-wise affine approximation for the deformation y and element-wise constant one for the other variables, by introducing

$$\begin{aligned} \mathcal{U}_d &\equiv \{v \in C(\bar{\omega}; \mathbb{R}^3) \colon v|_K \in P_0 \text{ for each } K \in \mathcal{T}_d,\ v = y_0 \text{ on } \Gamma\}, \\ \mathcal{V}_d &\equiv \{v \colon \omega \to \mathbb{R}^3 \colon v|_K \in P_0 \text{ for each } K \in \mathcal{T}_d\}, \\ \mathcal{W}_d &\equiv \{v \colon \omega \to [0,1] \colon v|_K \in P_0 \text{ for each } K \in \mathcal{T}_d\}, \end{aligned} \tag{37}$$

where $d > 0$ is the discretization parameter and $\mathcal{T}_d$ a triangulation of the reference domain ω.

Hence, the numerical minimization problem written in terms of the variables y, b, a, n, c and λ is

$$\begin{aligned} \text{Minimize} \quad & \mathcal{J}_{R_1}(y, b, a, n, c, \lambda) \\ \text{subject to} \quad & y \in \mathcal{U}_d, \\ & b, a, n, c \in \mathcal{V}_d, \\ & n \cdot e_3 = 0, \\ & \lambda \in \mathcal{W}_d, \end{aligned} \tag{38}$$

where the total free energy takes the form

$$\int_\omega \left\{ \lambda\varphi((y_{,1}|y_{,2}|b) - (1-\lambda)(a \otimes n + c \otimes e_3)) + (1-\lambda)\varphi((y_{,1}|y_{,2}|b) + \lambda(a \otimes n + c \otimes e_3)) \right\} \mathrm{d}x, \tag{39}$$

following from (31) for $k = 1$.

4.2 Tension and Compression Experiment for a Ni-Mn-Ga Single Crystal

Let us consider the Ni_2MnGa alloy and demonstrate using the numerical scheme described above the predicted austenite-martensite interface.

This alloy exhibits a cubic-to-tetragonal phase transformation with martensitic wells $U_1 = \mathrm{diag}(\nu_1, \nu_2, \nu_2)$, $U_2 = \mathrm{diag}(\nu_2, \nu_1, \nu_2)$, $U_3 = \mathrm{diag}(\nu_2, \nu_2, \nu_1)$ for lattice parameters $\nu_1 = 1.13$, $\nu_2 = 0.9512$, and is modelled by a St. Venant–Kirchhoff type free energy density

$$\varphi(F) = \min_{i=0,\dots,3} \varphi_i(F) = \min_{i=0,\dots,3} \frac{1}{2}(F - U_i) \cdot \mathbb{C}^i (F - U_i) \tag{40}$$

for all $F \in \mathbb{R}^{3\times 3}$, where the tensors of elastic moduli $\mathbb{C}^i$ take—using the Voigt notation—the values $\mathbb{C}^0_{11} = 13.6$ GPa, $\mathbb{C}^0_{12} = 9.2$ GPa, $\mathbb{C}^0_{44} = 10.2$ GPa for the austenite and $\mathbb{C}^i_{11} = 136$ GPa, $\mathbb{C}^i_{12} = 92$ GPa, $\mathbb{C}^i_{44} = 102$ GPa, $i = 1, 2, 3$, equally for all martensitic variants, inspired by the work of Kružík and Roubíček (2004).

In both the tension and compression experiments as reference configuration $\omega = (0, 9) \times (0, 4)$ is taken in the stress-free austenitic phase, cf. Figure 2 prescribing zero displacement Dirichlet boundary condition on Γ_{id}. On Γ_{pre} we have prescribed a given elongation.

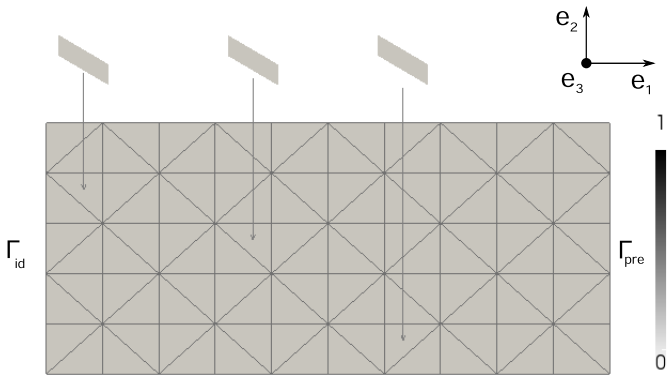

Figure 2: Reference configuration of Ni_2MnGa single crystal thin film in stress-free austenite (white)—Γ_{id} fixed boundary segment, Γ_{pre} boundary segment with prescribed elongation

The first-order laminate is, however, capable only of capturing two phase variants, therefore we had to select the competing wells with the greatest impact on the behaviour of the specimen, in our cases these were the austenite U_0 and the martensitic variant $U_1 = \mathrm{diag}(\nu_1, \nu_2, \nu_2)$, resp. $U_2 = \mathrm{diag}(\nu_2, \nu_1, \nu_2)$ for the tension, resp. compression test.

The minimization procedure has been done with the aid of the limited memory L-BFGS-B routine—developed by Byrd et al. (1995)—which is, however, designed for local optimization. Therefore, a successful computation of our global minimization problem, being, moreover, non-convex, is a challanging task which requires a good initial guess of the variables—involving the explicit computation of the interface between compatible wells. Afterwards, the visualization of the different fractions of the martensitic variants was completed by evaluating

$$\gamma(K) = \sum_{l=0}^{1} \lambda_l \frac{|(A_l^K)^T A_l^K - U_i^T U_i|^2}{|(A_l^K)^T A_l^K - U_0^T U_0|^2 + |(A_l^K)^T A_l^K - U_i^T U_i|^2} \tag{41}$$

on each element K of the triangulation with $\lambda_0 = \lambda$ and $\lambda_1 = 1 - \lambda$, then interpolating on the black–white scale as seen on Figure 3 and Figure 4 (the austenite is coloured white, the martensite black).

Note that as a result of the simplied model we used, the first-order laminate and the method of prescribing the elongation on Γ_{pre}, the elements at the fixed boundary parts cannot undergo phase transformation. Therefore Figure 3 exhibits certain unnatural symmetries in the volume fraction of the martensite—the austenite–martensite transformation is known to start in a corner of the specimen. However, our simulation was able to recover the nonlinear response of the material, specific for SMAs, under strain, cf. the stess–strain plot in Figure 3.

The compression experiment in Figure 4 shows a specific feature of thin films not observed in the bulk. When compressed, under a small back pressure, they bulge up without changing phase, i.e., the material persists in the austenite. This buckling effect has been proposed in Bhattacharya and James (1999), here simulated explicitly, and predicts that some theoretical tools, e.g., the non-buckling-type assumption (3.18) in Mielke and Roubíček (2003), might be natural in the bulk, but are never in the thin-film theory and should be avoided.

Another specific type of buckling related to the microactuation character of shape-memory alloys has been numerically investigated by Dondl et al. (2007).

5 Conclusion

The aim of this contribution was to draw attention to the difference between the modelling of bulk and thin film shape-memory materials with particular stress on richer structure of interfaces in some alloys, which first appeared in Bhattacharya and James (1999).

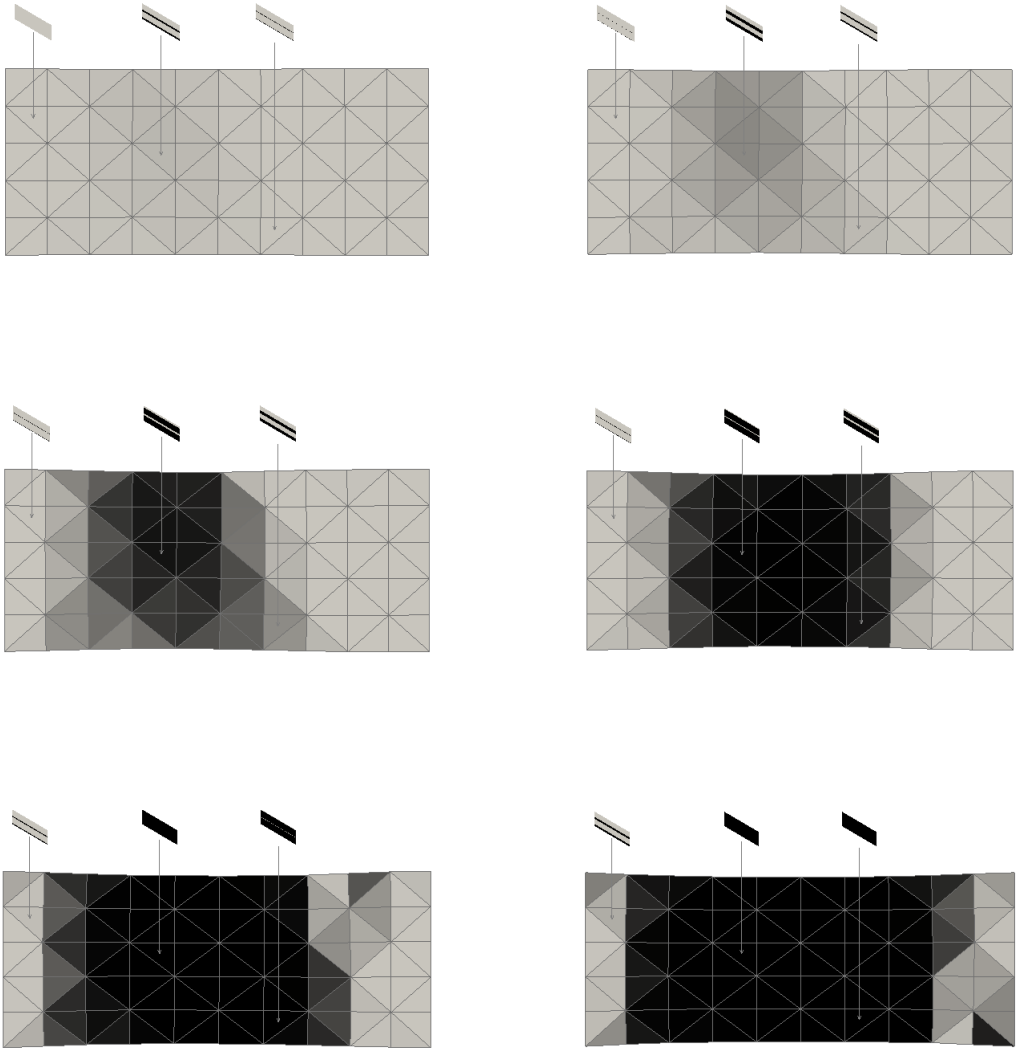

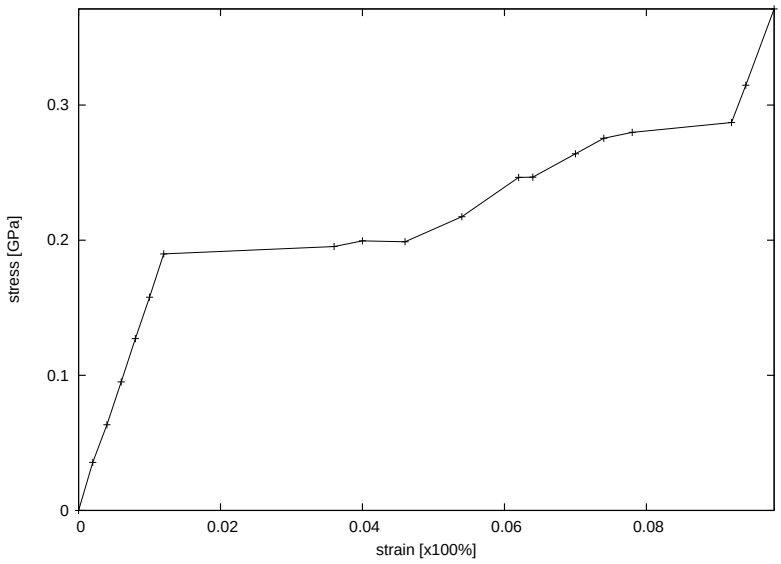

Figure 3: Tension experiment for Ni_2MnGa single crystal with 1, 2, 4, 6, 8 and 10% elongation in the x-direction and its stress–strain curve

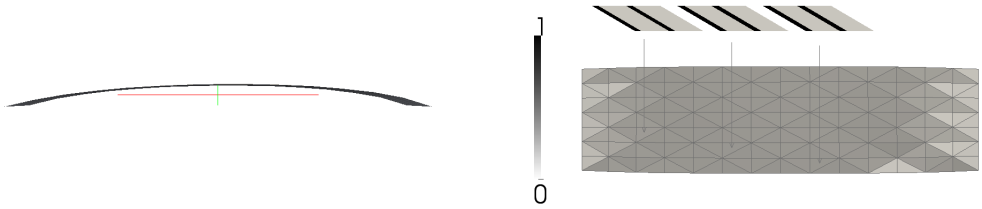

Figure 4: Side and top view on a 2% compressed Ni_2MnGa single crystal sheet with small back pressure exhibiting buckling with negligible phase transformation

To this behalf, after a brief overview of the different approaches to the derivation of a 2D model we have done some simple numerical calculations on an academic SMA alloy to justify the theoretical tools introduced.

As already pointed out before, a gradient-based optimization algorithm is not the most effective way to treat the non-convex minimization problem related to SMAs which usually possesses many local minima. Another interesting concept is to adopt a global optimization routine, e.g., particle swarm optimization (PSO), cf. Benešová (2011) for some promising results in 3D. However, these metaheuristic algorithms, such as the PSO and other genetic algorithms, do not guarantee that an optimal solution is ever found at all. Cf. Yang (2008) for an extensive overview of the topic.

Other future work will focus on the evolutionary problems in the thin film theory of shape-memory alloys which lacks an effective description till nowadays, the numerical method described above could then be easily extended to the dissipative evolutionary model.

Acknowledgement The author wishes to thank GA ČR for the support through the grant P105/11/0411 and MFF UK for the support through the project SVV-2011-263310 (GAUK ČR).

References

Benešová, B.: Global optimization numerical strategies for rate-independent processes. *J. Global Optim.*, 50, (2011), 197–220.

Bhattacharya, K.; James, R. D.: A theory of thin films of martensitic materials with applications to microactuators. *J. Mech. Phys. Solids*, 47, (1999), 531–576.

Bocea, M.: Young measure minimizers in the asymptotic analysis of thin films. *Sixth Mississippi State Conference on Differential Equations and Computational Simulations; Electron. J. Diff. Eqns., Conf.*, 15, (2007), 41–50.

Bocea, M.: A justification of the theory of martensitic thin films in the absence of an interfacial energy. *J. Math. Anal. Appl.*, 342, (2008), 485–496.

Bocea, M.; Fonseca, I.: Equi-integrability results for 3d-2d dimension reduction problems. *ESAIM: Control, Optimisation and Calculus of Variations*, 7, (2002), 443–470.

Braides, A.; Zeppieri, C.: A note on equiintegrability in dimension reduction problems. *Calc. Var. Partial Differential Equations*, 29, (2007), 231–238.

Byrd, R. H.; Lu, P.; Nocedal, J.; Zhu, C.: A limited memory algorithm for bound constrained optimization. *SIAM J. Sci. Comput.*, 16, (1995), 1190–1208.

Dacorogna, B.: *Direct Method in the Calculus of Variations*. Springer, Berlin (1989).

Dondl, P. W.; Shen, C. P.; Bhattacharya, K.: Computational analysis of martensitic thin films using subdivision surfaces. *Int. J. Num. Meth. Eng.*, 72, (2007), 72–94.

Freddi, L.; Paroni, R.: The energy density of martensitic thin films via dimension reduction. *Interface. Free Bound.*, 6, (2004), 439–459.

Friesecke, G.; James, R. D.; Müller, S.: A hierarchy of plate models derived from nonlinear elasticity by gamma-convergence. *Arch. Rational Mech. Anal.*, 180, (2006), 183–236.

Kinderlehrer, D.; Pedregal, P.: Gradient young measures generated by sequences in sobolev spaces. *J. Geom. Analysis*, 4, (1994), 59–90.

Kohn, R.; Strang, G.: Optimal design and relaxation of variational problems i, ii, iii. *Comm. Pure Appl. Math.*, 39, (1986), 113 – 137, 139 – 182, 353 – 357.

Kružík, M.; Roubíček, T.: Mesoscopic model of microstructure evolution in shape memory alloys with application to nimnga. *Preprint IMA No. 2003, Univ. of Minnesota, Minneapolis*.

Le Dret, H.; Raoult, A.: The nonlinear membrane model as variational limit of nonlinear three-dimensional elasticity. *J. Math. Pures Appl.*, 74, (1995), 549–578.

Mielke, A.; Roubíček, T.: Rate-independent model of inelastic behaviour of shape-memory alloys. *Multiscale Model. Simul.*, 1, (2003), 571–597.

Miyazaki, S.; Fu, Y. Q.; Huang, W. M.: *Thin Film Shape Memory Alloys: Fundamentals and Device Applications*. Cambridge University Press, New York (2009).

Müller, S.: Variational model for microstructure and phase transition. *In: S. Hildebrandt et al. (eds) Lecture Notes in Mathematics, Springer Berlin/Heidelberg*, 1713, (1999), 85–210.

Pan, Q.; Cho, C.: The investigation of a shape memory alloy micro-damper for MEMS applications. *Sensors*, 7, (2007), 1887–1900.

Pedregal, P.: *Parameterized Measures and Variational Principles*. Birkhäuser, Basel (1997).

Roubíček, T.: *Relaxation in Optimization Theory and Variational Calculus*. W. de Gruyter, Berlin (1997).

Shu, Y. C.: Heterogenenous thin films of martensitic materials. *Arch. Rational Mech. Anal*, 153, (2000), 39–90.

Šittner, P.; Novák, V.: Slitiny s tvarovou pamětí. *Technik*, 10, (2002), 23–32.

Yang, X. S.: *Nature-Inspired Metaheuristic Algorithms*. Luniver Press (2008).

Address: Mgr. Gabriel Pathó, Mathematical Institute, Charles Univesity in Prague, Sokolovská 83, CZ-186 75 Praha 8, Czech Republic and Faculty of Civil Engineering, Czech Technical University, Thákurova 7, CZ-166 29 Praha 6, Czech Republic.
email: g.patho@gmail.com.